

A New Drone-Borne GPR for Soil Moisture Mapping

Kaijun Wu, Gabriela Arambulo Rodriguez, Marjana Zajc,
Elodie Jacquemin, Michiels Clément and Sébastien Lambot
Louvain Georadar Research Centre (GPRLouvain), Earth and Life Institute,
Université catholique de Louvain
Louvain-la-Neuve, Belgium
kaijun.wu@student.uclouvain.be,
sebastien.lambot@uclouvain.be

Abstract—We present a new drone-borne ground-penetrating radar (GPR) for soil moisture mapping. The GPR system is lightweight, <1.5 kg, and consists of a vector network analyzer (VNA) as frequency-domain radar, a hybrid horn-dipole antenna operating in the range 250-2800 MHz, a microcomputer for controlling the radar, a smartphone or tablet for remote control, and a GPS for positioning. Radar data processing is performed using full-wave inversion based on the method of Lambot et al. As a proof of concept, we present the results of a data acquisition over an agricultural field in Saint-Denis, Belgium. For this example, we used the 500-700 MHz frequency range and inversion was performed in the time domain, focusing on the soil surface reflection. The retrieved permittivity was converted into soil moisture values using Topp’s equation. The soil moisture map was constructed using kriging. The obtained results were very consistent with the soil topography map, with higher soil moisture values observed in the talwegs and lower values observed in the highest slopes. Although the method still requires a few improvements before being routinely applicable, the method appears to be very flexible and promising for a series of drone applications, including precision agriculture and environmental engineering.

Index Terms—Drone, ground-penetrating radar, GPR, full-wave inversion, soil water content

I. INTRODUCTION

Drone technology has been developed rapidly over the past few years and has been used in a series of applications such as aerial photography, architecture, precision agriculture, security etc. [1]. It has also been used in the field of telecommunications and microwave imaging (e.g., [2], [3]). For underground detection, a commercial ground-penetrating radar (GPR) set up on a drone was used to determine snow thickness [4]. Using a drone-borne time-domain GPR was proven to be useful for landmine detection [5].

In the area of agricultural and environmental engineering, knowledge of soil moisture is of paramount importance (e.g., [6], [7]). In that respect, GPR has demonstrated to be a useful tool to provide soil moisture information with a high resolution at the field scale. A recent review summarizes soil moisture estimation methods using GPR [8], including recent developments of on- and off-ground measurements, corresponding instrumentation and data processing methods. According to petrophysics, the volumetric soil water content (SWC) can be obtained from the dielectric permittivity [9], [10], which can be derived from GPR. However, the application of drone-borne GPR for soil moisture estimation is still rare. Drone-borne GPR has the potential to reduce soil moisture mapping

works and expenses and, moreover, does not impact the soil and plants during the growing season.

In that framework, an off-ground configuration and a lightweight radar system are needed. A lightweight transverse electromagnetic (TEM) horn antenna with ultra-wideband structure is easy to construct because it simply consists of two metal plates [11], [12]. The full-wave inversion method is suitable [13]–[17] from the reasons that it is inherently that most accurate approach and moreover, it permits fully automated processing.

In this study, we set up a new air-borne, frequency-domain GPR using a lightweight vector network analyzer (VNA), a homemade hybrid horn-dipole antenna, a microcomputer and a remote controlling application. A GPS is used for positioning within the field. Data processing is based on full-wave inverse modeling in the time domain, focusing on the surface reflection only [13]–[15]. In that respect, the drone-radar-antenna system was characterized through its global reflection and transmission functions. Model fitting during inversion was made through a look-up table (LUT) for robust and real-time inversion. The drone-GPR data acquisitions were performed in an agricultural field located in Saint-Denis, Belgium. In order to assess the consistency of the soil moisture results, we also provide the elevation map and an orthophotography of the area.

II. DRONE-BORNE GPR

The drone-radar system includes mainly two parts: the radar system and the drone with GPS positioning. Specifically, a new hybrid horn-dipole antenna was built in order to cover a wide range of frequencies (250-2800 MHz) and being lightweight. The same antenna was used as transmitter and receiver. The impedance variation (50Ω at the feed point to $120\pi \Omega$ in the free space) within the antenna was tuned to be linear in the horn part. The design of the horn part of the antenna is presented in [12]. The antenna was directly connected to the reflection port of a 1-port handheld VNA (R60, Copper Mountain Technologies, USA), thereby setting up a stepped-frequency continuous-wave system. An Intel Computer Stick was used as controlling computer with user programs written with COM technology. The operating system is Windows 10. In addition, we developed Python and Javascript programs to remotely control the radar measurements, e.g., using a smartphone. A local Wi-Fi network is launched by the microcomputer with an external USB module, providing the user

interface with an HTTP server. The whole drone-borne GPR weight 1480 g and its size is $460 \times 126 \times 175$ mm. Figure 1 shows the radar prototype mounted on the drone during acquisitions. The drone is the X8 model from RCTakeOff, which is made of 8 motors and 4 arms (2 motors per arm).



Fig. 1. Prototype drone-GPR and drone for soil moisture mapping.

III. DATA PROCESSING

A. Radar equation and calibration

The radar signal was modeled using the radar equation developed by Lambot et al. [13], [15]. In the so-called far-field conditions applying to the drone-GPR configuration [18], namely, the distance between the antenna and the ground is larger than 1.2 the size of the antenna aperture [19], this radar equation is expressed in the frequency domain as:

$$S_{11} = H_i(\omega) + \frac{H(\omega)G_{xx}^\uparrow(\omega)}{1 - G_{xx}^\uparrow(\omega)H_f(\omega)} \quad (1)$$

In this equation, $S_{11}(\omega)$ is the reflection coefficient measured by the VNA, with ω being the angular frequency; $H_i(\omega)$ and $H_f(\omega)$ are the antenna complex global reflection coefficients of the antenna for the fields incident from the VNA and the ground, respectively, and $H(\omega)$ is the transmitting and receiving complex global transmission coefficient of the antenna. These three latter functions are characteristic to the drone-radar-antenna system and are determined through a calibration procedure. Finally, $G_{xx}^\uparrow(\omega)$ is the Green's function representing the backscattered electric field evaluated at the antenna phase center assuming a unit-source for wave propagation in a 3D layered medium [13], [20]. More details regarding the parameterization of this radar equation can be found in [13], [15]. It is worth noting that for accounting for the drone-radar interactions, calibration should be performed using the radar mounted on the drone.

B. Full-wave inversion

Inversion is formulated using the least squares problem and the objective function is accordingly defined as:

$$\phi(\mathbf{b}) = (\mathbf{g}_{xx}^{\uparrow*}(t) - \mathbf{g}_{xx}^\uparrow(t))^T (\mathbf{g}_{xx}^{\uparrow*}(t) - \mathbf{g}_{xx}^\uparrow(t)) \quad (2)$$

where $\mathbf{g}_{xx}^{\uparrow*}(t)$ and $\mathbf{g}_{xx}^\uparrow(t)$ are the time-domain, measured and modeled Green's function vectors, respectively. The measured Green's function is calculated from the radar measurements using Equ. (1). The parameter vector to be estimated is $\mathbf{b} = [h_0, \varepsilon_r]$, with h_0 being the distance between the antenna

phase centre and the soil surface and ε_r being the relative dielectric permittivity of the soil assumed as a half-space medium. This latter assumption can be made by focusing inversion on the surface reflection only, providing that it is not affected by the eventual presence of a thin layer [21]. Important to note as well is that the electrical conductivity of the soil is assumed to have a negligible effect on the surface reflection, which is valid in the frequency range dealt with in this study [14]. The effects of the soil slope and antenna tilting were neglected in this study, assuming as a first approximation that the antenna radiation pattern was uniform in the variation range of the angle. Nevertheless, for future applications, this should be accounted for.

Given the limited number of parameters to estimate, optimization of the objective function is made by computing it completely through the use of a pre-calculated look-up table (LUT) in the parameter space of interest [22]–[24]. Once the LUT is computed, this method has the advantage of being robust and extremely fast compared to the use of a gradient-based or global optimization method, namely, real-time inversion can be made. In this study, the LUT parameter vectors were defined as $\mathbf{h}_0 = [0.5 \ 6]$ m with intervals of 0.005 m and $\varepsilon_r = [2 \ 30]$ with the intervals of 0.5, resulting in a 1101×57 LUT (i.e., 62757 values).

IV. RESULTS

The measurements presented in this paper were performed over a bare, loamy agricultural field in Saint-Denis, in the region of Gembloux, Belgium (see Fig. 2). The size of the test field was 1.395 ha. In this particular analysis, we reduced the frequency range to 500-700 MHz, to which corresponds a depth of influence, considered as characterization depth, of about 10-20 cm. In this frequency range, the effect of soil surface roughness was negligible [25]. In total, 2437 radar measurements were collected over the field.

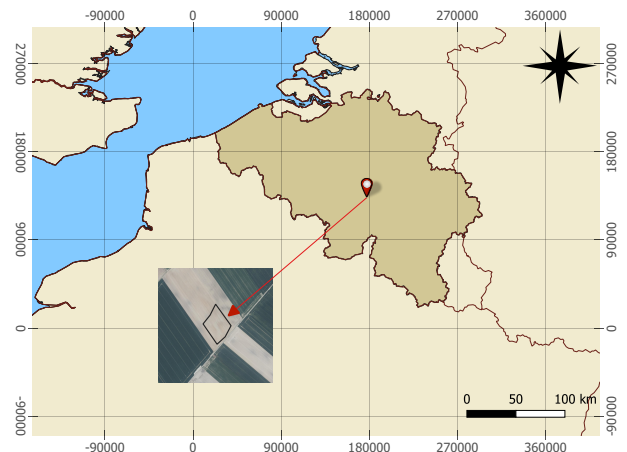


Fig. 2. The location of the study site: agricultural field in Saint-Denis (Belgium).

The petrophysical relation between the relative dielectric permittivity ε_r and the soil moisture of Topp [9] was used to derive the volumetric soil moisture θ for each measurement point:

$$\theta = -5.3 \times 10^{-2} + 2.92 \times 10^{-2} \varepsilon_r - 5.5 \times 10^{-4} \varepsilon_r^2 + 4.3 \times 10^{-6} \varepsilon_r^3 \quad (3)$$

The kriging interpolation method was used to get the soil water content map from the GPR point measurements. To provide insights into the consistency of the obtained soil moisture map, we compare the results with the digital elevation model of the plot as well as with an orthophotography (see Fig. 3). Both were obtained from aerial photographs using photogrammetry.

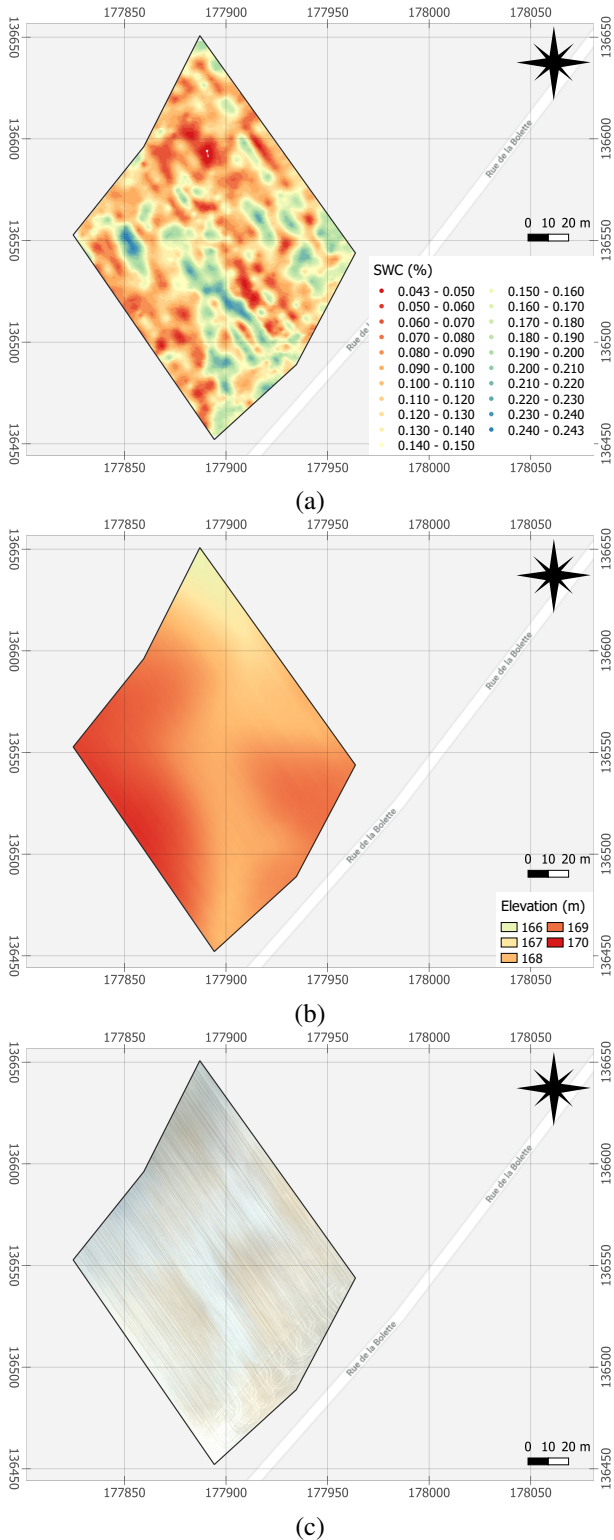


Fig. 3. Agricultural field in Saint-Denis, Belgium. (a) Volumetric soil moisture derived from the drone-GPR measurements, (b) digital elevation model and (c) soil orthophotography.

As we can see in the elevation map (Fig.3(b)), this field presents a gentle topography with a talweg, slight slopes and flat areas. Soil topography is one of the major factors governing soil moisture distribution in the field, together with soil texture. Regarding this later factor, the orthophotography (Fig.3(b)) shows different soil colors that are correlated to surface soil texture distributions, with the whiter areas corresponding to silt accumulated through erosion in the talweg and darker areas containing more clay and carbon content.

As shown in the soil moisture map (Fig.3(a)), there is mostly a wet area extending from the southern part of the field to its centre and a drier area in the south-western part of the field. In general, the soil moisture map is quite consistent with the distribution from the soil topography. A good correlation is also observed with the soil color map. It is worth noting that both the plateau and talweg are relatively flat, leading both to the same incidence angle, and present contrasted moisture levels. This indicates that for this field, it is indeed expected that neglecting the incidence angle was a relatively good approximation.

V. CONCLUSION

A lightweight radar system was designed to be mounted on a drone for soil moisture mapping. Full-wave inversion is used to determine the soil water content from the radar data, which theoretically provides the best possible estimates. For fast inversion, a LUT-based approach was adopted. We used kriging interpolation to obtain the soil moisture map. The comparison with the digital elevation map and real soil picture greatly confirms the potential of this technology. Our future works will focus on (1) the calibration of the full-wave radar model for accounting for different incidence angles resulting from drone tilting and variable soil topography, (2) improving the antenna design for improved signal-to-noise ratio, and (3) validation using comparisons with ground-truths.

ACKNOWLEDGMENTS

This research was funded by the Politique Scientifique Fédérale (BELSPO, Belgium) in the frame of the Research Programme for Earth Observation STEREO III, RAPAS project (contract SR/00/238) and the Fonds de la Recherche Scientifique (FNRS, Belgium). This research was also carried out within the framework of EU COST Action TU 1208 "Civil Engineering Applications of Ground Penetrating Radar".

REFERENCES

- [1] D. Floreano and R. J. Wood, "Science, technology and the future of small autonomous drones," *Nature*, vol. 521, no. 7553, pp. 460–466, 2015.
- [2] G. Fasano, A. Renga, A. R. Vetrella, G. Ludeno, I. Catapano, and F. Soldovieri, "Proof of concept of micro-uav-based radar imaging." Institute of Electrical and Electronics Engineers Inc., 2017, Conference Proceedings, pp. 1316–1323.
- [3] G. Ludeno, I. Catapano, A. Renga, A. R. Vetrella, G. Fasano, and F. Soldovieri, "Assessment of a micro-uav system for microwave tomography radar imaging," *Remote Sensing of Environment*, vol. 212, pp. 90–102, 2018.
- [4] H. Machguth, O. Eisen, F. Paul, and M. Hoelzle, "Strong spatial variability of snow accumulation observed with helicopter-borne gpr on two adjacent alpine glaciers," *Geophysical Research Letters*, vol. 33, no. 13, 2006.
- [5] D. Šipoš, P. Planinšič, and D. Gleich, "On drone ground penetrating radar for landmine detection," in *2017 1st International Conference on Landmine: Detection, Clearance and Legislations, LDCL 2017*, Conference Proceedings, pp. 7–10.

- [6] H. Vereecken, J. A. Huisman, H. Bogaert, J. Vanderborght, J. A. Vrugt, and J. W. Hopmans, "On the value of soil moisture measurements in vadose zone hydrology: A review," *Water Resources Research*, vol. 46, no. 4, 2010.
- [7] H. Vereecken, M. Aitkenhead, S. Allison, S. Assouline, P. Baveye, M. Berli, N. Brüggemann, P. Finke, M. Flury, T. Gaiser, G. Govers, A. Schnepf, T. Ghezzehei, P. Hallett, H. Hendricks Franssen, J. Heppell, R. Horn, J. Huisman, D. Jacques, F. Jonard, S. Kollet, F. Lafolie, J. Hopmans, K. Lamorski, D. Leitner, A. McBratney, B. Minasny, C. Montzka, W. Nowak, Y. Pachepsky, J. Padarian, N. Romano, K. Roth, M. Javaux, Y. Rothfuss, E. Rowe, A. Schwen, J. Šimůnek, A. Tiktak, J. Van Dam, S. van der Zee, H. Vogel, J. Vrugt, T. Wöhling, D. Or, I. Young, T. Roose, J. Vanderborght, M. Young, and W. Amelung, "Modeling soil processes: Review, key challenges, and new perspectives," *Vadose Zone Journal*, vol. 15, no. 5, 2016.
- [8] A. Klotzsche, F. Jonard, M. C. Looms, J. van der Kruk, and J. A. Huisman, "Measuring soil water content with ground penetrating radar: A decade of progress," *Vadose Zone Journal*, vol. 17, no. 1, 2018.
- [9] G. C. Topp, J. L. Davis, and A. P. Annan, "Electromagnetic determination of soil water content: Measurements in coaxial transmission lines," *Water Resources Research*, vol. 16, no. 3, pp. 574–582, 1980.
- [10] J. Ledieu, P. De Ridder, P. De Clerck, and S. Dautrebande, "A method of measuring soil moisture by time-domain reflectometry," *Journal of Hydrology*, vol. 88, no. 3-4, pp. 319–328, 1986.
- [11] A. R. Mallahzadeh and F. Karshenas, "Modified horn antenna for broadband applications," *Progress in Electromagnetics Research*, vol. 90, pp. 105–119, 2009.
- [12] J. Jezova, S. Lambot, A. Fedeli, and A. Randazzo, "Ground-penetrating radar for tree trunk investigation," in *2017 9th International Workshop on Advanced Ground Penetrating Radar, IWAGPR 2017 - Proceedings*, Conference Proceedings.
- [13] S. Lambot, E. C. Slob, I. D. Van Bosch, B. Stockbroeckx, and M. Vanclooster, "Modeling of ground-penetrating radar for accurate characterization of subsurface electric properties," *IEEE Transactions on Geoscience and Remote Sensing*, vol. 42, no. 11, pp. 2555–2568, 2004.
- [14] S. Lambot, L. Weihermüller, J. A. Huisman, H. Vereecken, M. Van-clooster, and E. C. Slob, "Analysis of air-launched ground-penetrating radar techniques to measure the soil surface water content," *Water Resources Research*, vol. 42, no. 11, 2006.
- [15] S. Lambot and F. André, "Full-wave modeling of near-field radar data for planar layered media reconstruction," *IEEE Transactions on Geoscience and Remote Sensing*, vol. 52, no. 5, pp. 2295–2303, 2014.
- [16] J. Minet, P. Bogaert, M. Vanclooster, and S. Lambot, "Validation of ground penetrating radar full-waveform inversion for field scale soil moisture mapping," *Journal of Hydrology*, vol. 424-425, pp. 112–123, 2012.
- [17] F. Jonard, L. Weihermüller, H. Vereecken, and S. Lambot, "Accounting for soil surface roughness in the inversion of ultrawideband off-ground gpr signal for soil moisture retrieval," *Geophysics*, vol. 77, no. 1, pp. H1–H7, 2012.
- [18] A. P. Tran, C. Warren, F. André, A. Giannopoulos, and S. Lambot, "Numerical evaluation of a full-wave antenna model for near-field applications," *Near Surface Geophysics*, vol. 11, no. 2, pp. 155–165, 2013.
- [19] A. P. Tran, F. André, C. Craeye, and S. Lambot, "Near-field or far-field full-wave ground penetrating radar modeling as a function of the antenna height above a planar layered medium," *Progress in Electromagnetics Research-Pier*, vol. 141, pp. 415–430, 2013.
- [20] E. Slob and J. Fokkema, "Coupling effects of two electric dipoles on an interface," *Radio Science*, vol. 37, no. 5, 2002.
- [21] J. Minet, S. Lambot, E. C. Slob, and M. Vanclooster, "Soil surface water content estimation by full-waveform gpr signal inversion in the presence of thin layers," *IEEE Transactions on Geoscience and Remote Sensing*, vol. 48, no. 3, pp. 1138–1150, 2010.
- [22] N. Rajaram, T. H. Nguyen, and J. W. Tunnell, "Lookup table-based inverse model for determining optical properties of turbid media," *Journal of Biomedical Optics*, vol. 13, no. 5, 2008.
- [23] J. P. Gastellu-Etchegorry, F. Gascon, and P. Estève, "An interpolation procedure for generalizing a look-up table inversion method," *Remote Sensing of Environment*, vol. 87, no. 1, pp. 55–71, 2003.
- [24] S. B. Kim, S. Huang, L. Tsang, J. Johnson, and E. Njoku, "Soil moisture retrieval over low-vegetation surfaces using time-series radar observations and a lookup table representation of forward scattering," in *International Geoscience and Remote Sensing Symposium (IGARSS)*, Conference Proceedings, pp. 146–149.
- [25] S. Lambot, M. Antoine, M. Vanclooster, and E. C. Slob, "Effect of soil roughness on the inversion of off-ground monostatic gpr signal for noninvasive quantification of soil properties," *Water Resources Research*, vol. 42, no. 3, 2006.